Society of Petroleum Engineers

SPE-185748-MS

Quantification of Recovery Factors in Downspaced Wells: Application to the Eagle Ford Shale

Saurabh Sinha and Deepak Devegowda, University of Oklahoma; Bhabesh Deka

This paper was prepared for presentation at the 2017 SPE Western Regional Meeting held in Bakersfield, California, USA, 23 April 2017.

Abstract

In this paper, we present the results of an elaborate simulation study from the Eagle Ford shale by integrating rate transient analysis (RTA), microseimic interpretation and rock typing to quantify the well recovery factors.

First,we builda fine-scale geocellular model to represent the lithology of Eagle Ford Shale (EFS)in interest. A fully compositional fluid model wasthen integrated into the geocellular model. The stimulated rock volume (SRV) is based on microseimic data interpretation. The permeability of the system is calibrated from rate transient analysis (RTA) using the methodology suggested by (Suliman et al. 2013). Historical production data of a 500'conventional spacing 3-well PAD is then matched and the sensitivity to well spacing is then carried out using the history-matched model in two configurations. These are same layer completions and staggered well completions. Recovery factors are then quantified with the help of expected ultimate recovery (EUR) calculated from simulation forecasts and original gas in place (OGIP) calculated with the help of volumetric calculation.

Our results show that the conventional 500'spacing is not optimal in the rich condensate area of the Eagle Ford shale. Additionally, there were little to no difference in the predicted EUR's in staggered or same layer completions. Microseismic data suggests that the fracture grows up to the top of EFS and is not limited to the lower EFS. We also perform sensitivity studies with respect to drawdown that show minimal or no condensate banking with choke management. Early-time condensate banking is however very sensitive to higher drawdown pressures.

Introduction

Hydraulic fracturing is a key enabling technology allowing for economic production from shale wells. Because of the ultra-low permeability of these plays, each well can behave as an individual unit with its own associated Stimulated-Reservoir-Volume (SRV) for an extended period. Therefore, placing wells too far apart means inefficient drainage of the reservoir. Conversely, closer well placement can lead to inter-well rate interference (Ajani and Kelkar 2012). In both cases, however, the EUR's and hence the recovery factors must be quantified to optimally place newer wells andfor accurate reserves accounting.

Decline curve analysis (DCA) and analytical mathematical models (Stalgorova and Mattar 2013), although useful, provide an oversimplified picture of the the problem and do not consider the complexities of multiphase flow in shales. Also, such analytic methods are limited in terms of their ability to conduct elaborate sensitivity studies to determine governing factors on well or reservoir productivity. In this paper, we have tried to identify the key issues for the quantification of recovery factors in shales and deduce the best practices to drill, complete and produce from an unconventional rich condensate reservoir.

Description of the Geologic Model

The geologic model is constructed from five pilot well log suites that include gamma ray, sonic, neutron porosity, density and mineralogy logs. No core data is available for core to well log correlation. The location of the pilot wells and the PAD wells to be modelled is shown in Figure 1.

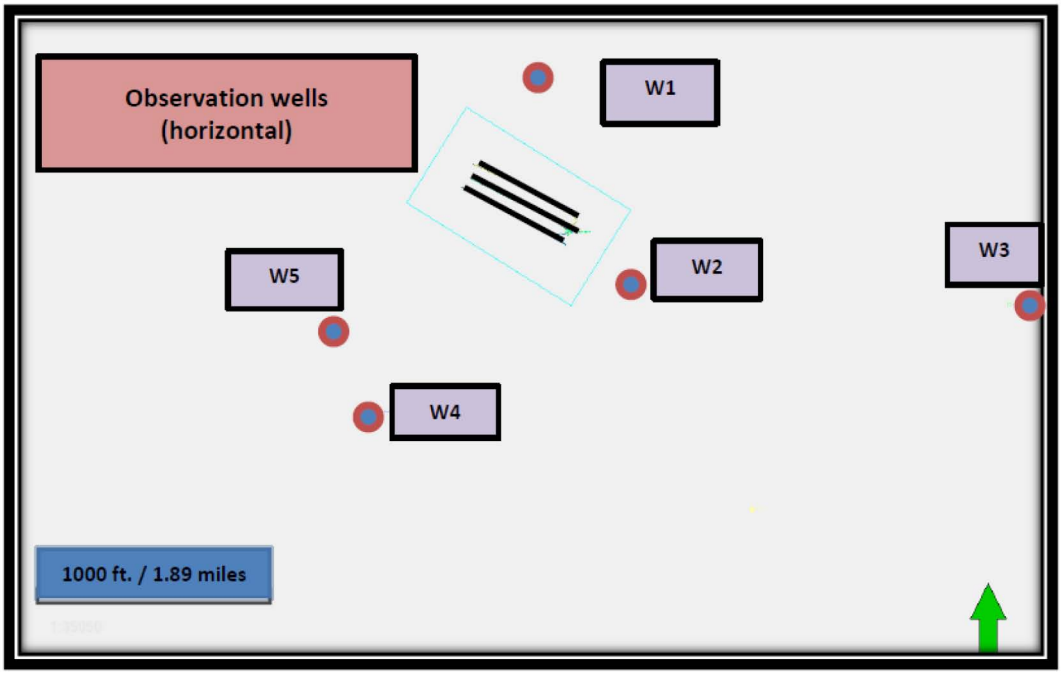

Figure 1—Observation wells and offset pilot well location (W1 to W5). Three wells on the PAD are shown in the figure as lines adjacent to each other. These wells are referred to as observation wells in the study (well 1, well 2 and well 3). Five wells in the vicinity are the pilot wells for which a full log suite is available. All petrophysical properties are calculated on pilot wells and are later interpolated using lithology constrained sequential Gaussian simulation (SGS) for observation wells.

Well Log Processing

Well logs are first processed by depth shifting and then applying correct temperature and pressure corrections. Porosity calculations relied on the use of neutron and density logs. Calculations of water saturation began with quantifying the mineralogy of the Eagle Ford in the study area. Figure 2 show the mineralogy of the EFS as documented by Sondhi (2013) using Fourier Transform Infrared Spectroscopy (FTIR) conducted on EFS core samples.

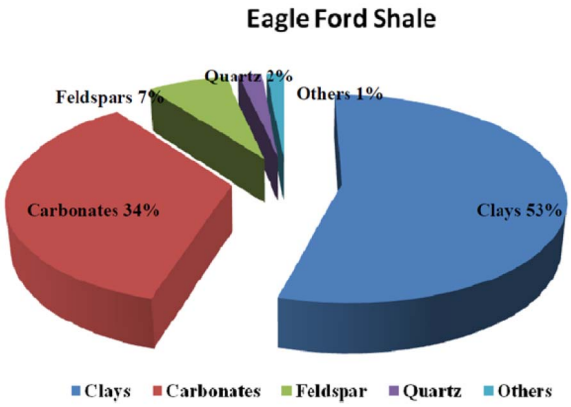

Figure 2—FTIR mineralogy given by Sondhi (2011). Eagle Ford mineralogy consist of mainly carbonate and clay with minor percentages of feldspar, quartz and other minerals.

Rock typing was performed using the gamma ray log and bulk density log and four different rock types (RC1, RC2, RC3 and RC4) were identified in this study.

Calculation of a, m and n parameters. Because the Eagle Ford shale is predominantly calcite and clay, we utilize the results from Hamada et al. (2010) who have documented Archie's parameters, a, m and n for this mineralogy as 0.28, 2.34 and 2.87 respectively. Water saturation was then calculated using Archie's, Simandoux', Total Shale, Waxman Smits and Indonesian Shale models. Figure 3 shows that the Simandoux equation (Doveton, 2001) gives reasonable results for water saturation and as expected calculations using Archie's equations are considerably high because of the high percentage of clays.

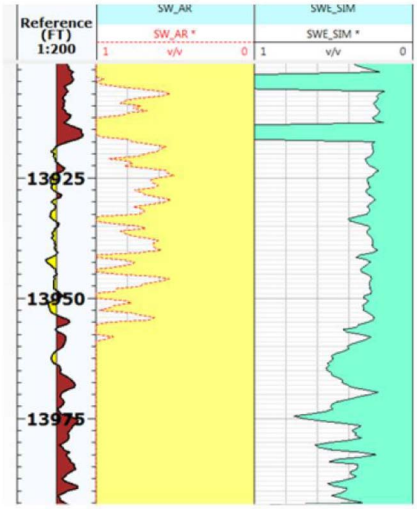

Figure 3—Water saturation calculation. Left to right on track: gamma ray, water saturation by Archie's equation and water saturation by Simandoux euation. Simandoux equation predicts reasonable results (20%-25%) for water saturation. The Archie equation is invalid in the presence of clays and shows close to 100% water saturation.

Stratigraphic and Structural Framework

The structural characteristics and lithological variations are integrated in to a detailed 3D model. Figure 4 shows the gamma ray log and the bulk density plots from 4 pilot well logs in the study. Three sequences S1, S2 and S3 or Upper, Middle and Lower EFS can be identified on the gamma ray and bulk density logs. Bulk density first decreases and then increases from the top of EFS (horizon 4) towards the bottom of EFS (horizon 1). Sharp spikes in gamma ray values may indicate high cyclic packages (Workman, 2013).

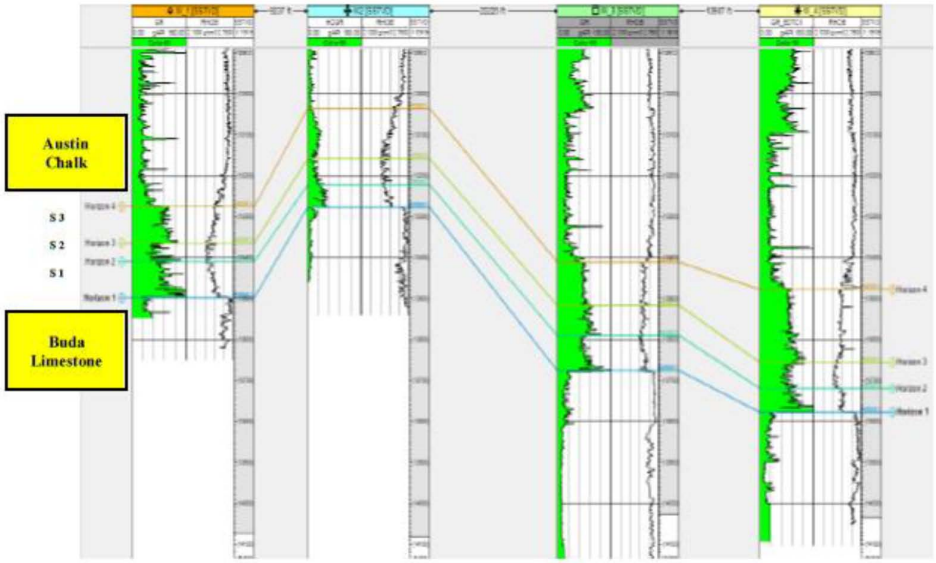

Figure 4—Cross section of 4 wells (W1-W4) on gamma ray and bulk density. Sequence 1(S1), Sequence 2(S2) and sequence 3(S3) can be identified on the gamma ray and bulk density log. Bulk density first decreases (transgressive phase) and then increases (regressive phase) from top of EFS towards bottom EFS. Spikes in gamma ray suggest high cyclic packages. Horizon 1 is the top of Buda limestone and Horizon 4 is the top of EFS. From left to right on track: Gamma ray (0-150 API), Bulk Density (2.1-2.75 g/cm3).

Assigning probability maps and variograms. To generate the probability maps, the thickness of all the rock types (RC1-RC4) is mapped in all intervals (Upper, Middle and Lower EFS). This average thickness is mapped in all zones to create average thickness probability maps per rock type. These probability maps are summarized in Appendix A for all zones and all rock types.

Spatial distribution of lithology

Sequential indicator simulation (SIS) is then used to model the 3D distribution of rock types in the study area. The variogram description is provided in Appendix A. Figure 5 shows the rock type variations determined along each of the 4 pilot wells.

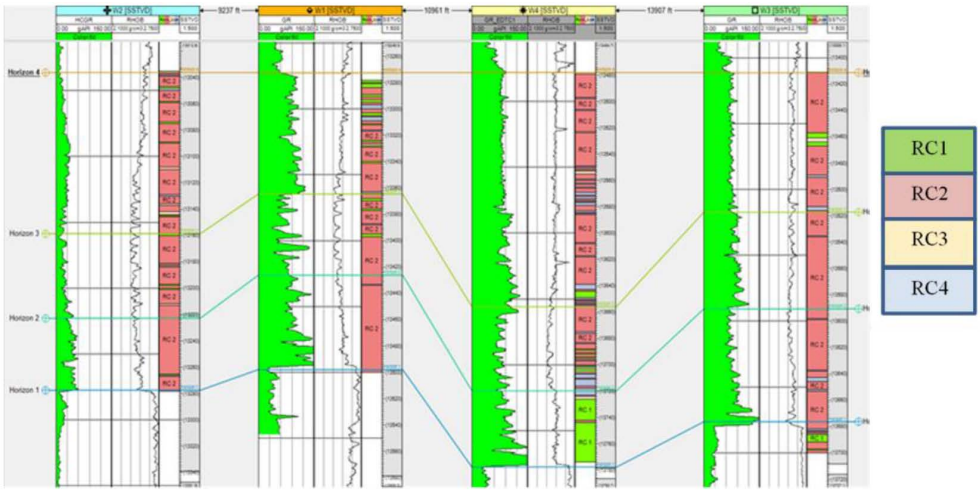

Figure 5—Cross section for 4 pilot well logs in the study. We observe from the cross section that Rock Type 1 and 2 are more continuous and are observed in all the wells in all zones. However, Rock Type 3 and 4 occur as small heterogeneities across all well logs. From left to right on the plot: Gamma ray log (0-150 API), bulk density (2.1-2.75 gm/cc) and rock types. Color associations for the rock typesare shown in the legend.

The number of layers in the three zones, Upper, Middle and Lower EFS is chosen based on the thickness of each zone. Figure 6 shows the final layering scheme along with the rock types / lithology in actual and upscaled logs. With the number of layers as 50, 25 and 50 in the Upper, Middle and Lower EFS respectively, all the subtle details in lithology are resolved and hence is chosen as final layering scheme for the static model. We finally modeled porosity and permeability variations across the model using sequential Gaussian simulation (SGS). The permeability at well locations is calculated using rate transient analysis (RTA). Appendix C shows the rate transient analysis results for three wells on the PAD used for simulation.

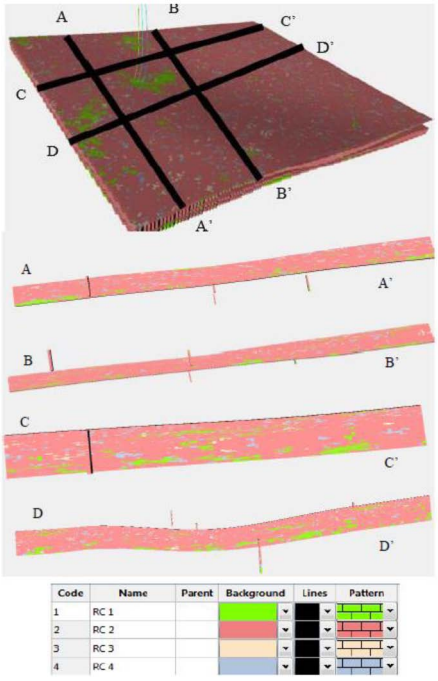

Figure 6—3D lithology model with north-south and east-west cross section. Rock type 1 and 2 are predominant in the lower Eagle Ford. Non- productive rock types (RC3 and 4) are present in middle and upper Eagle Ford. Color associations are consistent with the rock typing from Figure 5.

Fluid Modeling

For fluid modeling, we relied on the use of:

a. Separator oil and gas and mathematically recombined composition
b. Constant composition expansion (CCE) data
c. Gas depletion study at reservoir temperature of 330 deg. F

We have used the Equation-of-State calibration procedure described by Whitson (1983)and the results of the calibration are provided in Appendix B.

Simulation Study

Additional Model details

A single porosity model is chosen with fractures modeled using high permeability gridecells. The fracture network is determined by amplitude filtering microseismic events as described in (Suliman et al. 2013). Figure 7 shows the microseimic events after the amplitude filter and the amplitude range used in the analysis. The relative permeability curves are generated using correlations. Wells are coupled explicitly in the model and the well flowing bottomhole pressure(FBHP) is calculated from tubing head pressure (THP) using the Hagedorn and Brown correlation (Hagedorn and Brown 1965).

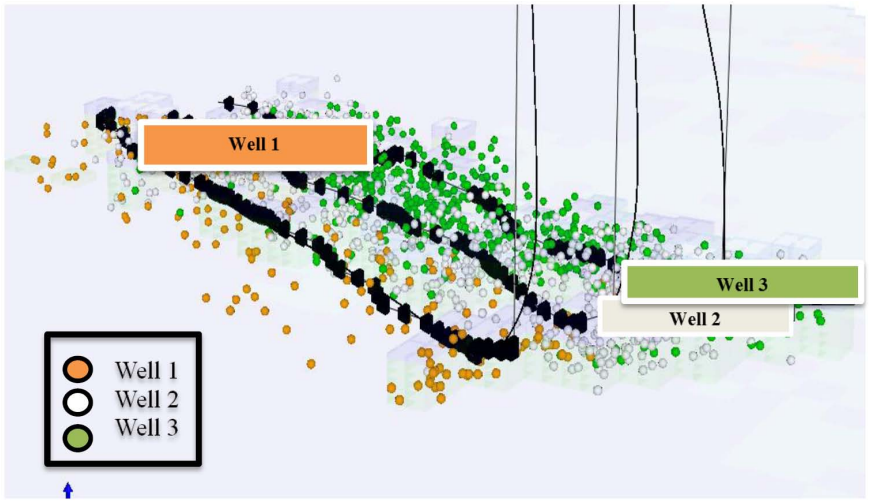

Figure 7—Well-by-wellhydraulic fracturing related microseismic events. Events associated with the wells are color coded with orange for well 1, white for well 2 and green for well three.

History Matching

The only history matching parameters used are the water saturations and the fracture network conductivity. The model is run on gas rate control and the condensate rate, FBHP and water rates are predicted. The simulation results are shown in Figure 8 for 500' basecase spacing.

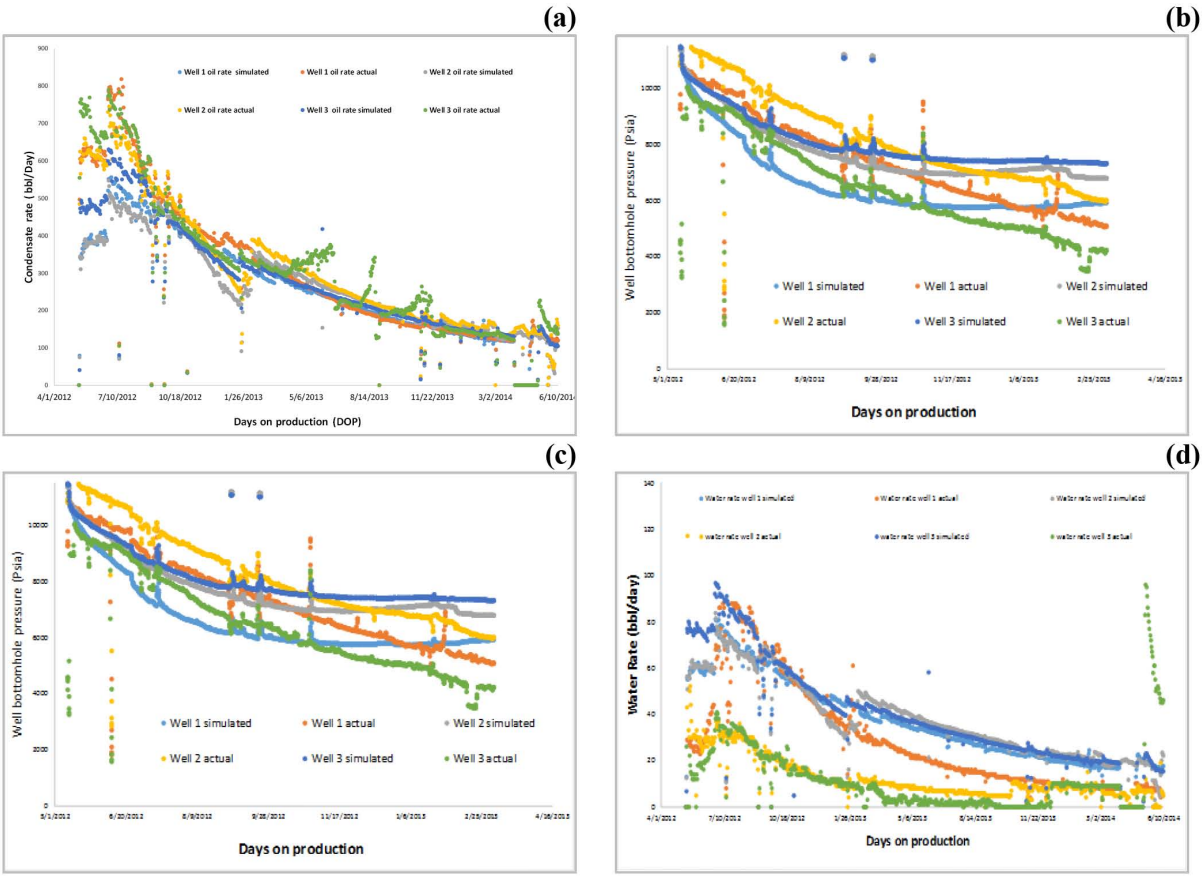

Figure 8—Summary of history matching results for all three wells on the PAD (actual and simulated). Model is run on gas rate control. Subplot (a) gives gas rates, (b) is oil rate, (c) is the well bottomhole pressure while (d) shows water rates as a function of time.

The model is run for a total of 30 years well life and the cumulative production at the end of well life is considered as expected ultimate recovery (EUR). For forecasting, the model is run on exit gas rates at the end of history matching to forecast rates in the future. Secondary constraints of 800 psi minimum bottomhole pressure (BHP) is used in the model.

Results from 500' Well Spacing Base Case Study

The following conclusions were obtained from the simulation study described earlier:

a. The middle well shows a higher SRV than the other two wells. The reason for this is illustrated in Figure 9.
b. The system behaves like a volumetric reservoir i.e. little or no contribution beyond the fracture tips. This can be observed in Figure 10.
c. GOR Trends: Figure 10 shows the gas oil ratio (GOR) trends of all wells. The early increase in GOR implies an early drop in reservoir pressure and hence early condensate banking effect. Early condensate banking means the condensate recovery in the well will suffer and hence it should be considered in the reserves accounting process. This is shown in Figure 11.

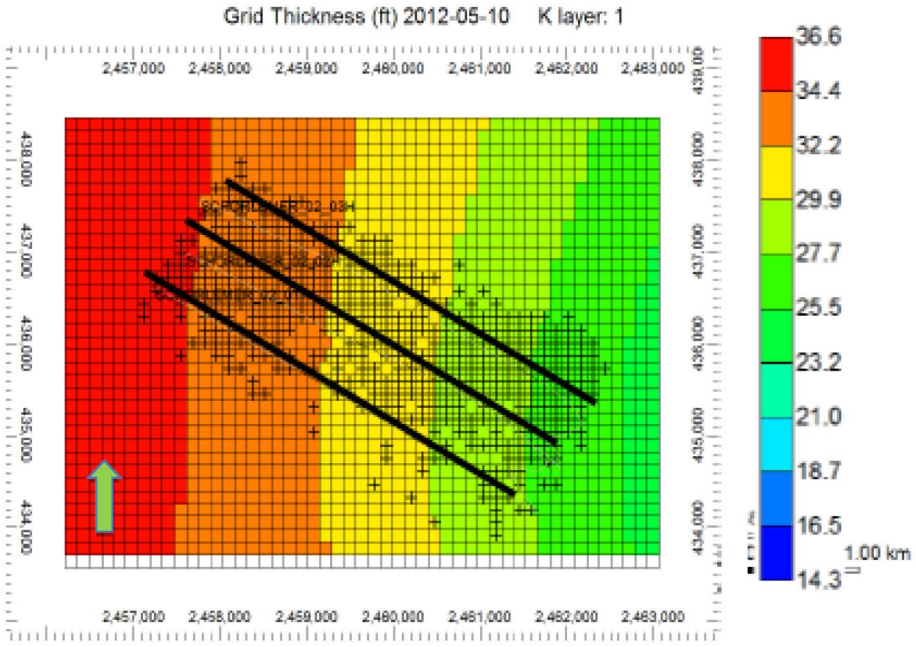

Figure 9—Fracture network assigned to wells. Fracture networks are represented in black crosses. Wells are represented by black lines. From left to right; well 1, well 2 and well 3. More stimulated rock volume (SRV) is available in the middle portion of the reservoir. On extreme left or extreme right of the 3 well PAD, there is less stimulation. Hence, a higher SRV is available for well 2 to drain. Also, the South East portion of the reservoir is the heel of the well and North West is the location of the toe of the wells. There is more stimulation towards heel versus the toe of the wells.

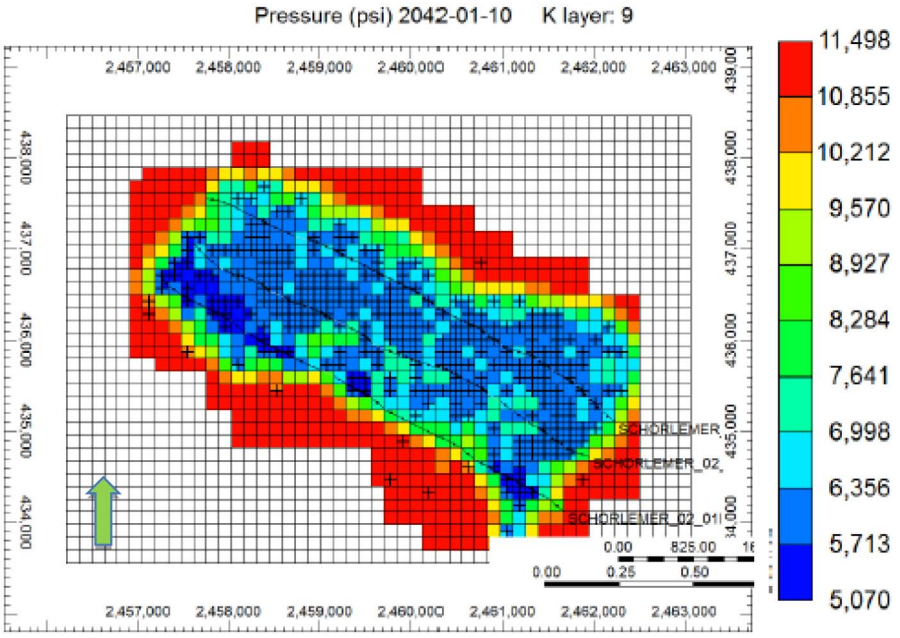

Figure 10—Pressure depletion in the reservoir at the end of well life. Uneven drainage areas can be observed across the reservoir. Comparison of this drainage area with the fracture network in Figure 9 indicates that reservoir drainage is restricted to the stimulated reservoir volume.

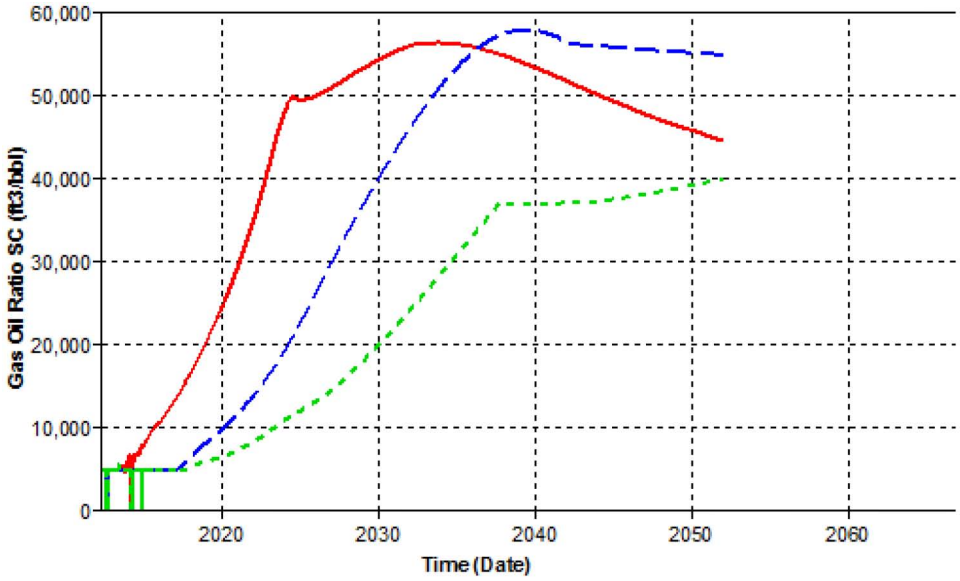

Figure 11—GOR trends for all wells on the PAD. It can be observed that GOR increases much earlier in well 1 (red curve) than well 2 or 3 (blue and green curves respectively). Hence, the dew point is reached earlier in the well with a smaller associated SRV. This implies that the same drawdown settings cannot be employed on all wells in the same PAD. Drawdown management should be individualized to the associated stimulated reservoir volume(SRV) in each well.

Well Spacing Sensitivities

Well spacing sensitivity studies in this work focuses on the use of two well configurations. These are wells completed in the same layer and wells placed a staggered fashion. These two scenarios are elaborated in Figures 12 and 13 respectively.

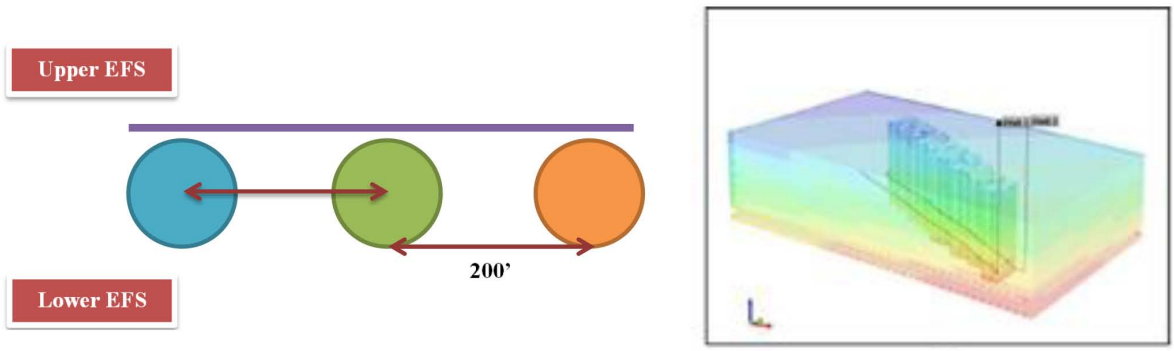

Figure 12—Example well configuration for same layer completion. All three wells are placed in lower Eagle Ford (EFS) section. Distance between two neighboring lower EFS wells is 200'.

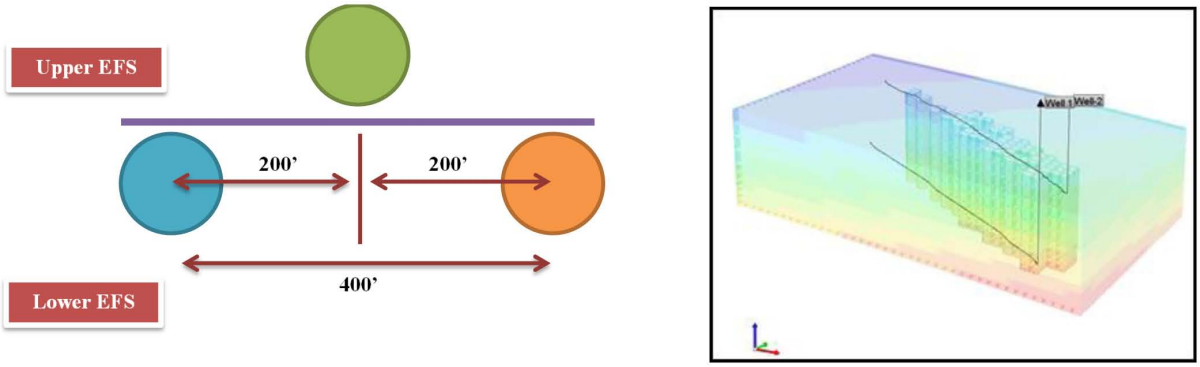

Figure 13—Example well configuration for staggered completion. Distance between adjacent lower Eagle Ford wells is 400'. Wells are less likely to be in rate interference in this configuration.

For our sensitivity studies, we assumed that the SRV associated with each well remains the same and is not a function of spacing. This need not necessarily be true; however, because we have not included stress-regime changes associated with the SRV, we utilize this assumption. Parameters used for volumetrics are described in appendix D. Results from well spacing sensitivity studies are summarized in Table 1. The recovery factor is shown to be maximum at 420' in both cases.

Table 1—Expected ultimate recovery (EUR) and recovery factor (RF) from same layer and staggered completions. The recovery factor is a maximum at a well spacing of 420' in both cases and hence is chosen to be the optimal spacing. Well lateral length is 5000' in all cases.

Same Layer				
Well Spacing	**Oil EUR**	**Gas EUR**	**OGIP(BSCF)**	**RF**
140	160	1.5	11	14%
280	250	3.6	22	16%
420	**480**	**5.8**	**33**	**18%**
700	440	5.4	39	14%
840	449	5.15	39	13%
980	465	5.35	39	14%
1120	435	5.1	39	13%
Staggered				
Well Spacing	**Oil EUR**	**Gas EUR**	**OGIP(BSCF)**	**RF**
140	115	1.1	11	10%
280	225	3.1	22	14%

Same Layer				
Well Spacing	**Oil EUR**	**Gas EUR**	**OGIP(BSCF)**	**RF**
420	**440**	**5.5**	**33**	**17%**
700	425	5.25	39	13%
840	445	5.35	39	14%
980	455	5.45	39	14%
1120	420	4.9	39	13%

Observations

a. Dramatic decrease in recovery factors for 140' and 280' case: In the 140' and 280' spacing there is a significant loss in EUR's due to downspacing. This is attributed to the fact that below certain well spacing values, the fracture conductivities may increase with increase in proppant volumes. However, the SRV remains the same. In downspaced wells, reducing the amount of proppant may therefore be one option to reduce the well cost while still being able to achieve the same EUR's.
b. Drilling all wells simultaneously to avoid future re-fracturing costs: Re-fracturing during development stage is often a necessary completion practice. Wells completed with single well PAD's, essentially act as pressure sink for newer hydraulic fracturing stages at adjacent wells and can therefore suffer a "fracture hit". This may especially be true for older wells that have drained a sufficiently larger volume. To avoid a ‘fracture hit’, it may be prudent to refracture the older wells first prior to completing a new well.
c. There was no discernable advantage to completing the wells using staggered completions.
d. Drawdowns must be managed in order to minimize condensate dropout. A shale well contained within its associated SRV acts as an isolated, volumetric reservoir with little contribution from outside the network. Drawdown management hence become even more important at smaller spacings and forms the focus of the next section.

Drawdown Management

To quantify the effect of drawdown management, wells with 280' well spacing are modeled with different drawdowns. A very fine scale grid refinement is used to capture both the pressure depletion and retrograde condensation around the grid blocks. The model has a fixed SRV of 3.7 E+08 ft^3 under different drawdown controls. The drawdown is increased gradually till retrograde condensation is observed.

The results 3 years in to well life and at the end of well life (30yrs) are summarized in Figure 14. With a drawdown value below 8000 psi, no condensate is observed around the wellbore even towards the end of well life. However, there is early condensate banking around the wellbore when drawdown exceeds 8000 psi. Hence, the well must be operated below this drawdown to avoid condensate banking.

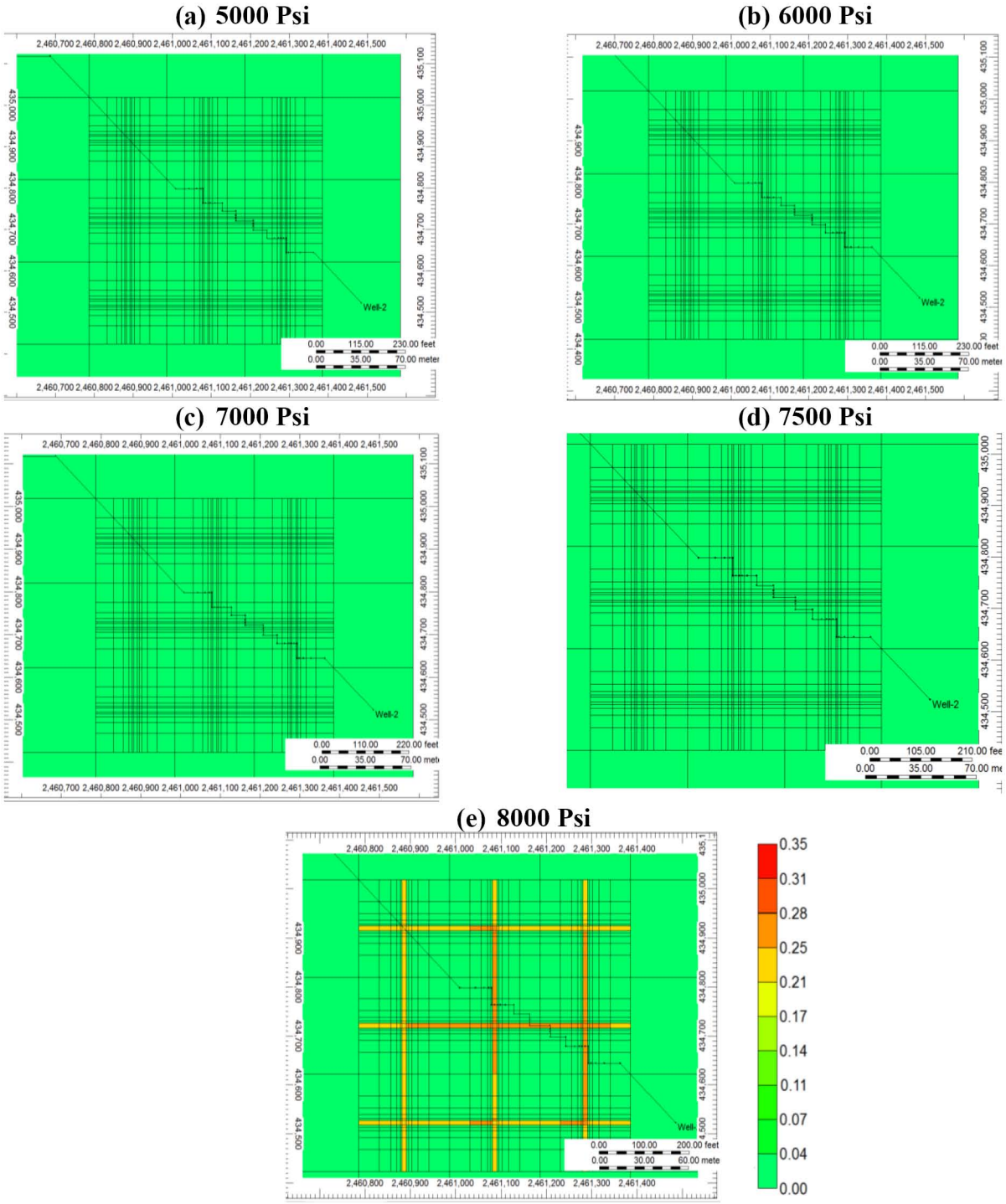

Figure 14—Oil saturation around the wellbore at different drawdowns at the end of 30 years in(a) to (d) and at the end of 3 years in figure (e). The well is shown as a line running from the right bottom corner to the top left corner of each diagram. The figures show (a) for a well operated under a constant drawdown of 5000 psi, (b) for well operated under a constant drawdown of 6000 psi, (c) for well operated under a constant drawdown of 7000 psi, (d) for well operated under constant drawdown of 7500 psi, (e) for well operated under a constant drawdown of 8000 psiat the end of 3 years. It can be observed that an early condensation occurs around the wellbore for a threshold drawdown of 8000 psi.

Conclusions

In our study, history matching of historical production data shows uneven drainage areas with more drainage on the heel side of the lateral. Sensitivities on the history matched model indicate that a well spacing of 420' maximizes the recovery factors and hence is the optimal well spacing. Sensitivities on staggered versus

same layer completions indicate that there is no significant difference in expected ultimate recoveries in staggered versus same layer completions.

Sensitivity studies on pressure drawdowns indicate that the reservoir behaves as a volumetric reservoirs and drawdowns must be tailored to the the stimulated rock volume(SRV) associated with each well. High drawdowns in smaller SRV's may lead to early condensate banking in the reservoir.

Acknowledgement

We would like to thank K Patel and Tanh Nguyen from computer modeling group Ltd. for technical support for this project.

Nomenclature

EUR : Expected ultimate recovery
RTA : Rate transient analysis
EOS : Equation of state
CCE : Constant composition experiment
DCA : Decline curve analysis

References

Ajani, Ayantayo Abdulkamil, and Mohan Gajanan Kelkar. 2012. "Interference Study in Shale Plays." SPE Hydraulic Fracturing Technology Conference, no. February: 6–8. doi:10.2118/151045-MS.

Doveton, John H. 2001. "*All Models Are Wrong, but Some Models Are Useful: 'Solving' the Simandoux Equation Prolog: The Archie Equation*."

Hagedorn, Alton, and Kermit Brown. 1965. "Experimental Study of Pressure Gradients Occurring During Continuous Two-Phase Flow in Small-Diameter Vertical Conduits." *Journal of Petroleum Technology* 17: 475–84. doi:10.2118/940-PA.

Hamada, G M, The British, A A Almajed, and King Fahd. 2010. "*Uncertainly Analysis of Archie S Parameters Determination Techniques in Carbonate Reservoirs Calculation of Archie S Parameters*," 1–10.

Sondhi, Namrita. 2013. "Petrophysical Characterization of Eagle Ford Shale." *Journal of Chemical Information and Modeling* **53** (9): 1689–99. doi:10.1017/CBO9781107415324.004.

Stalgorova, Ekaterina, and Louis Mattar. 2013. "*Analytical Model for Unconventional Multifractured Composite Systems*," no. August.

Suliman, B., R. Meek, R. Hull, H. Bello, D. Portis, and P. Richmond. 2013. "*Variable Stimulated Reservoir Volume (SRV) Simulation: Eagle Ford Shale Case Study*." Spe 164546, 13. doi:10.2118/164546-MS.

Whitson, Curtis H. 1983. "Characterizing Hydrocarbon Plus Fractions." *Society of Petroleum Engineers Journal* **23** (4): 683–94. doi:http://dx.doi.org/10.2118/12233-PA.

Appendix A

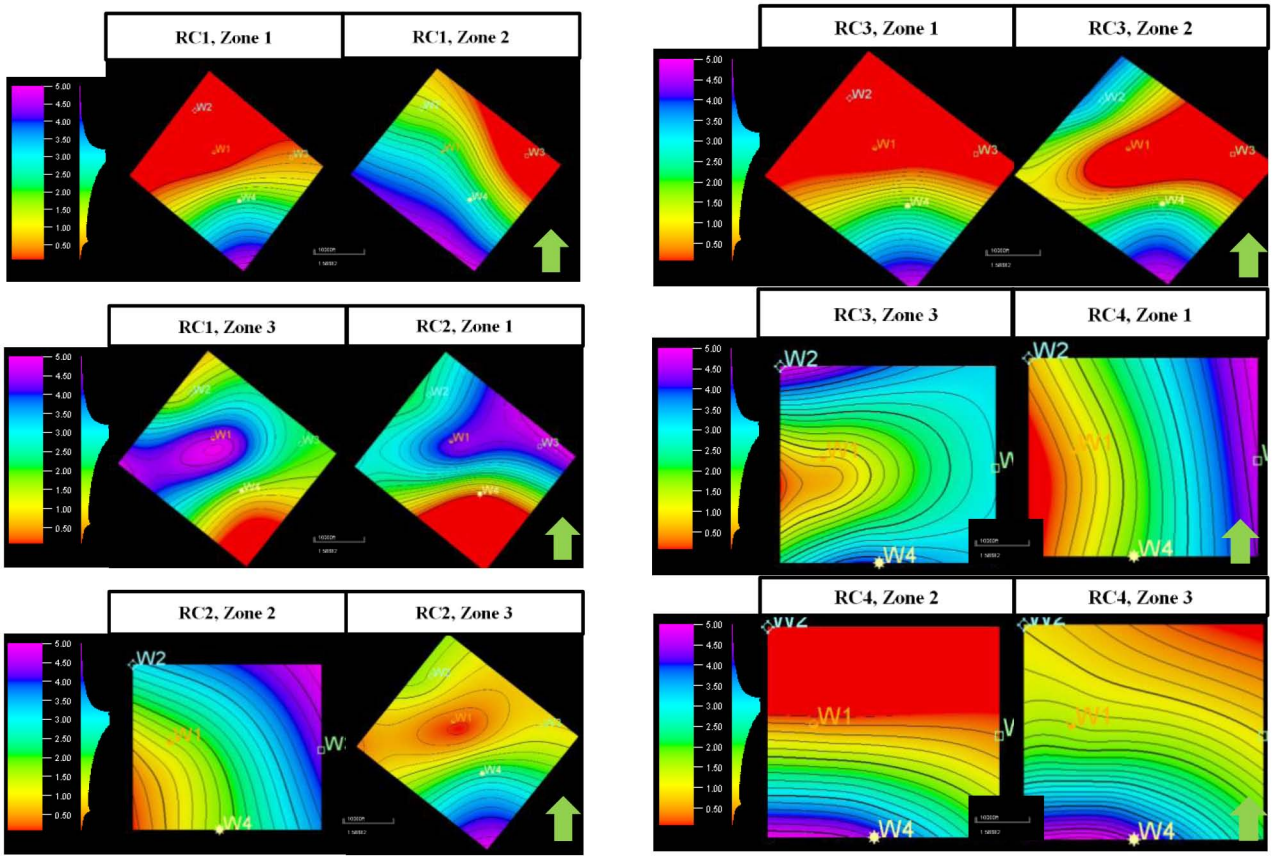

Figure A1—Thickness probability map for rock types 1 −4 in all zones. Rock type 1 and 2 are predominant with a directional trend that is modeled with an anisotropic variogram.

Appendix B

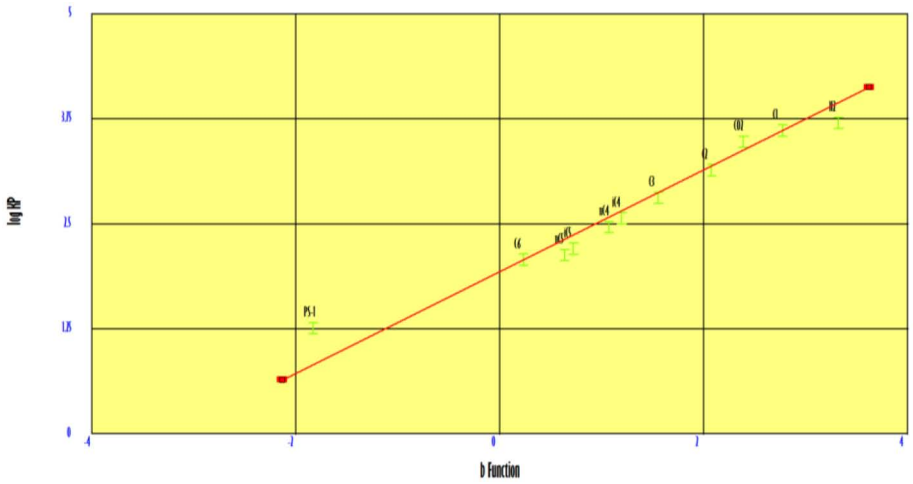

Figure B1—Hoffman quality plot. The green markers represent different components from the PVT report and the red curve represents the ideal curve. It can be observed that the components honor the ideal curve and hence fluid pass the quality check.

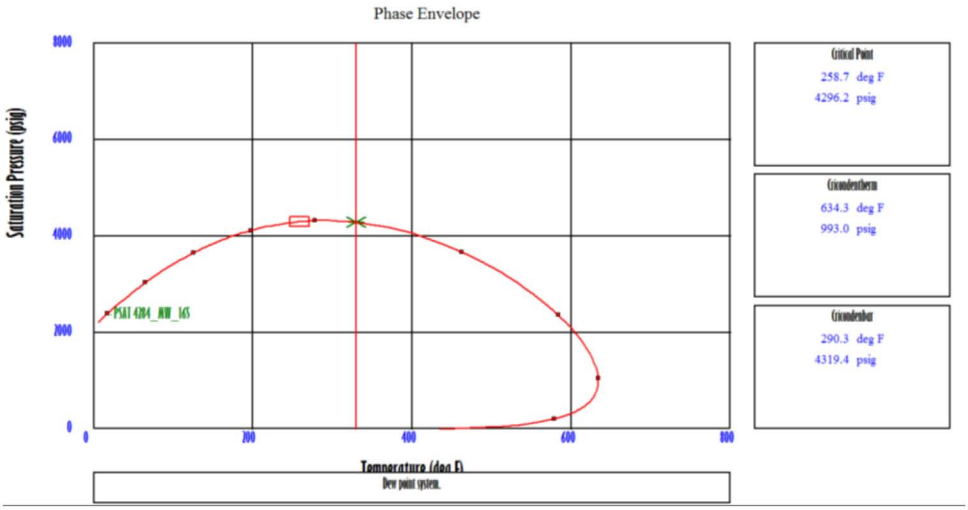

Figure B2—Initial phase envelope with 6 pure components and 1 plus fraction. Red curve shows the phase envelope of the fluid system after reducing the molecular weight. On X axis is the reservoir temperature and on the Y axis is the reservoir pressure. Solid vertical red line represents the reservoir temperature of 330-degree F. Green symbol represents the dew point pressure of 4284 Psi and the red symbol represents the critical point of the symbol. As the reservoir temperature lies between critical point and cricondentherm, the reservoir fluid is a retrograde gas condensate system.

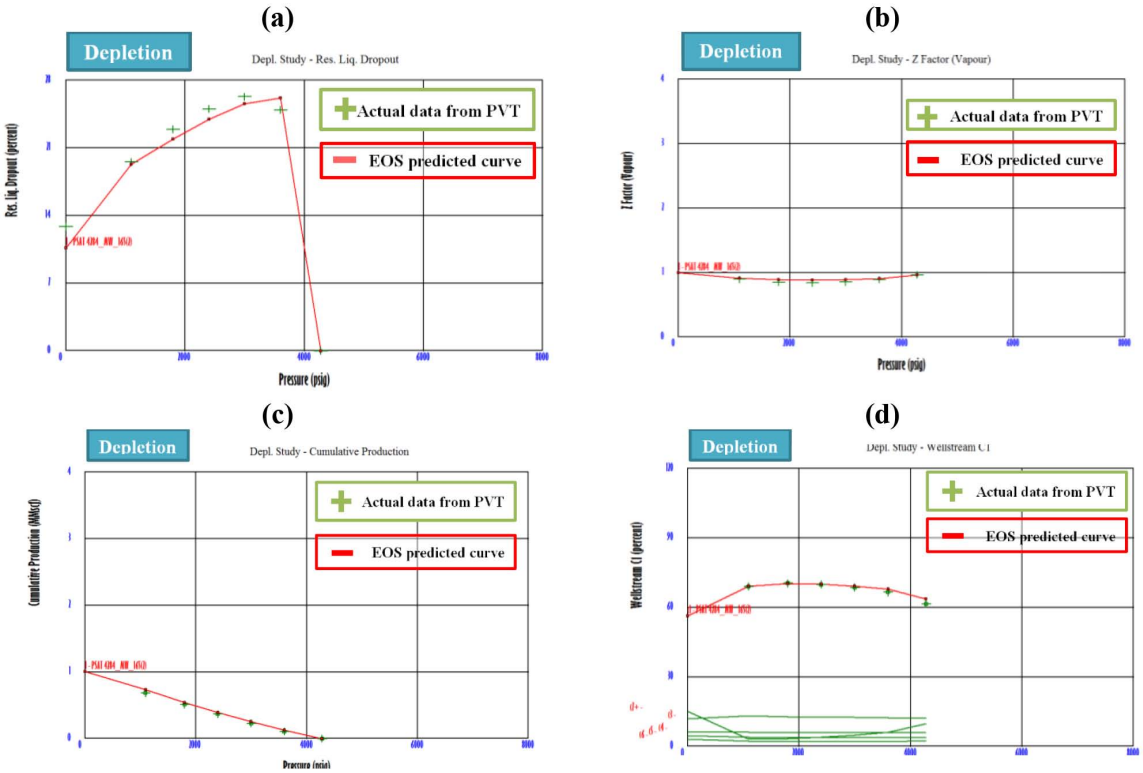

Figure B3—Key results from final lumped composition from equation of state (EOS) modeling and the final lumping scheme used. The green crosses indicate actual PVT data points and the red curve indicate the fit from EOS. a) Reservoir liquid droput curve from gas depletion experiment b) Z factor from depletion experiment c) Cummulative production from depletion experiment d) Wellstream production of C1 from depletion experiment.

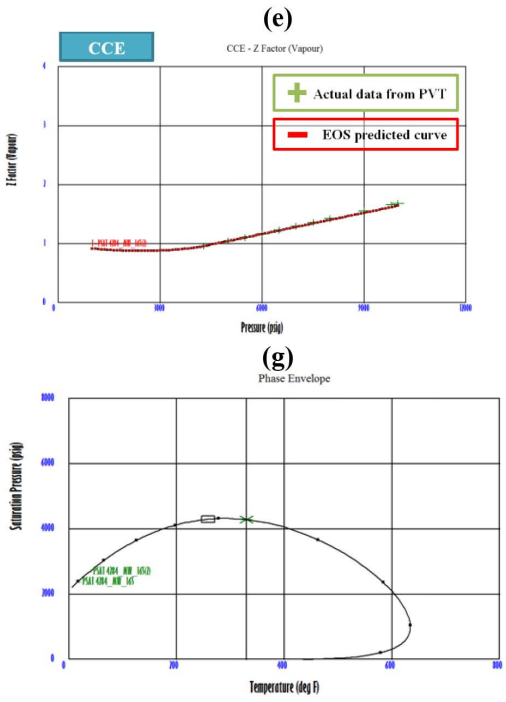

N2 + C1
CO2 + C2 + C3
iC4 + nC4 + iC5 + nC5 + C6
C7::C7 + C8::C8 + C9::C9
C10::C10 + C11::C11
C12::C13 + C14::C15
C16::C17 + C18::C20 + LAST_PSEUDO

Figure B4—Key results from final lumped composition from equation of state (EOS) modeling and the final lumping scheme used. The green crosses indicate actual PVT data points and the red curve indicate the fit from EOS.e) Z factor from constant composition expansion (CCE) experiment f) Relative volume from CCE experiment g) Phase envelope from lumped composition.

Appendix C

Table C1—Results summary from RTA for all the wells on the PAD.

Parameter	Well1	Well 2	Well 3
Time end of linear flow (t_{elf}), days	70.0	135.0	142.0
Dimensionless fracture conductivity(F_{cd})	896.6	1000.0	533.9
Product of drainage area and square root permeability ($A_c k^{1/2}$),md$^{1/2}$	83510.0	71893.0	70411.1
Matrix permeability (k), md	5.19E-05	1.18E-05	1.16E-05
Fracture half length (X_f), ft.	186.0	227.0	248.0
Expected ultimate recovery (EUR), gas BSCF	1.5	2.1	1.9
Original gas in place (OGIP), gas BSCF	8.1	10.7	10.1
Recovery factor (RF), gas percentage	19.0	19.7	18.4
Drainage area (A_{srv}),Acres	37.0	44.0	51.0

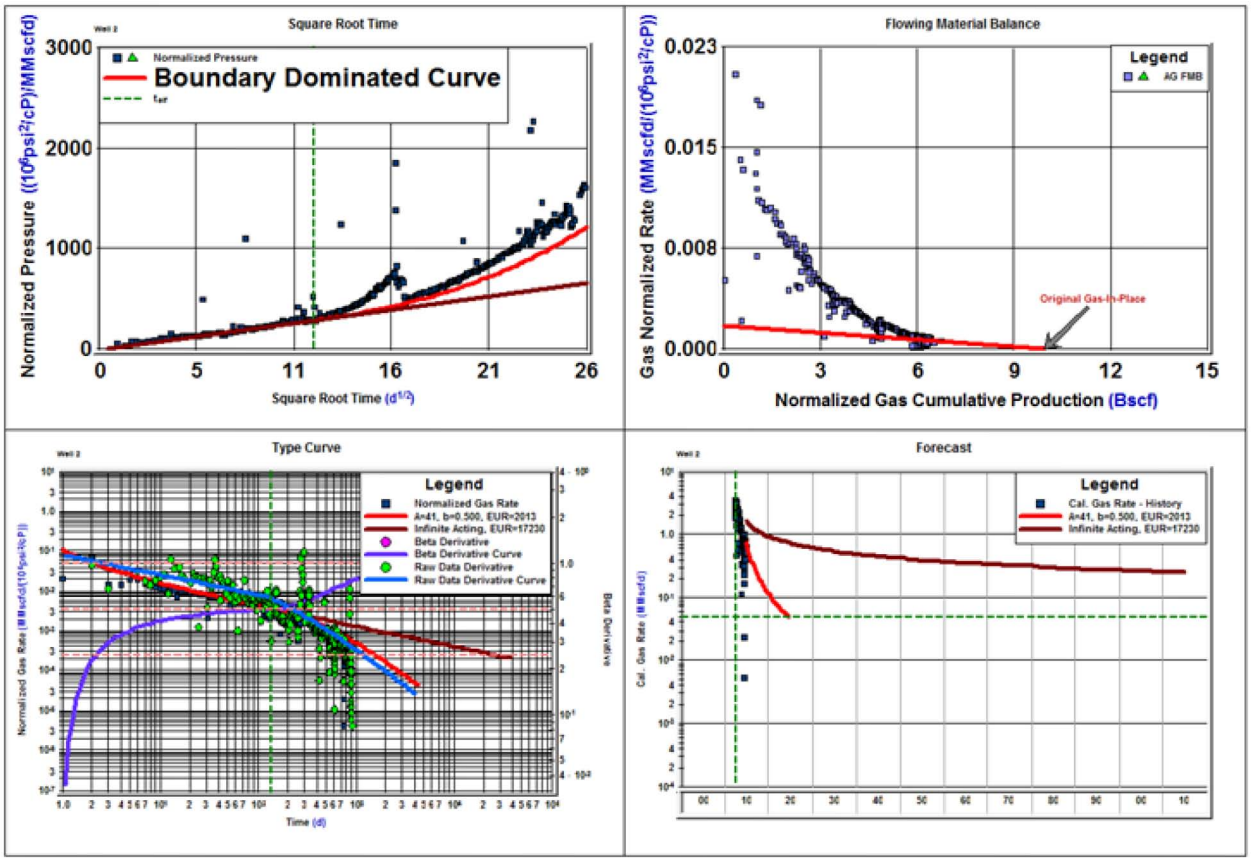

Figure C1—Example LFA summary from one well from PAD (well 2). From left to right first plot is square root time plot used to identify end of linear flow and calculate time end of linear flow (t_{elf}). Second plot is the flowing material balance plot used to calculate original gas in place(OGIP). Plot on bottom left is the normalized gas rate (forecast plot) along with type curve. Last plot (bottom right) is the forecast plot. Matrix permeability derived from LFA is distributed log normally in the static model.

Appendix D

To calculate the original gas in place, we have used the volumetric equation as:

$$G = \frac{Ah\varphi S_{gi}}{22.957\ B_{gi}}$$

Where, G is the original gas in place, A is Area (acres), h is the pay zone thickness (ft), S_{gi} is the initial water saturation, and B_{gi} is the initial gas formation factor. The volumetric parameters used and the results from the 500' spacingcase study are summarized in Table D1 and D2.

Table D1—Result summary from 500' history matched basecase.

Well	1	2	3	Avg.
SRV (ft3)	4.80E+08	6.80E+08	6.25E+08	5.95E+08
Fracture conductivity	1000	1000	1000	1000
Fracture Width	0.01	0.01	0.01	0.01
Effective Permeability (mD)	1	1	1	1
Oil EUR (MSTB)	420	450	430	433
Gas EUR(BSCF)	4.9	5.4	5.2	5.2
OGIP, BSCF	39	39	39	39
Gas RF	13%	14%	13%	13%
Drainage Area (acres)	50	71	65	62

Table D2—Parametrs used for volumetrics to calculate the original gas in place (OGIP).

Parameter	Value	Source
Area	57 ac	Calculated with 500 ft. well spacing and a fixed lateral length of 5000 ft.
Pay	220 ft.	Well logs
Porosity	10%	Median value from the simulation model
Initial water saturation	0.8	Median value from well logs
Initial Gas formation volume Bg	1.113	From PVT report
Final OGIP	39 Bscf	Calculated

Results for the 500' spacing case are described in table. It can be observed in the table that the average SRV from 3 wells is 5.95 E+08. However, the SRV for a 5000' lateral is only 4.62 E+08 Ft. Hence, it is a fair assumption that all the area between the wells with less than 420' will be drained completely if the completion is same. This scenario is shown in Figure D1.

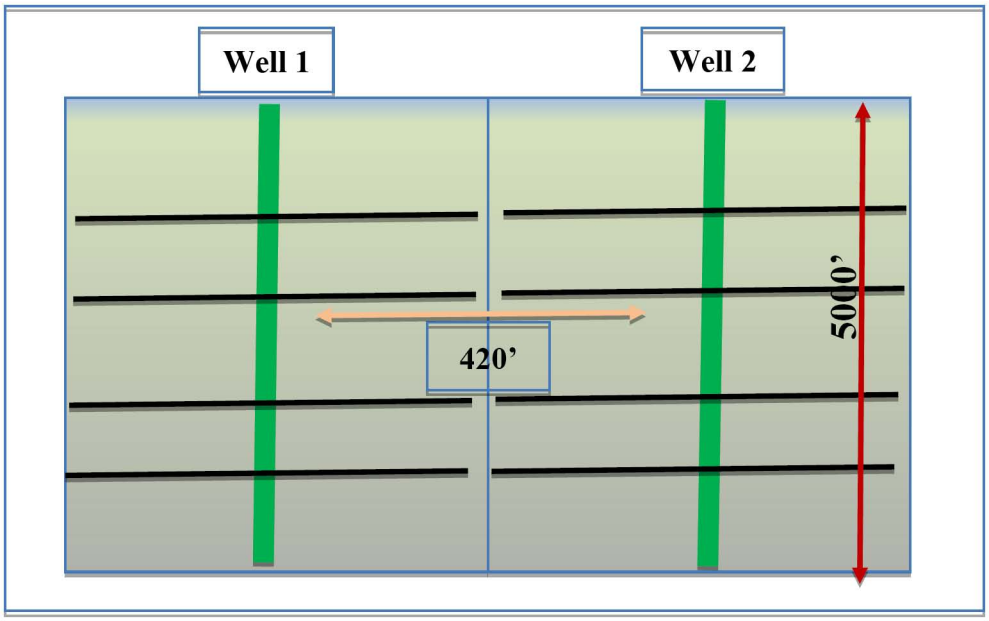

Figure D1—Drainage scenario for downspaced wells with 420' well spacing. The maximum drainage area is shown by the square rectangular green boxes. The fractures shown in black just touch each other. The SRV for this case is: (lateral length) *(well spacing)* pay thickness = 5000'420'*220'=4.62E+08 < 5.95 E+08 (average SRV for basecase study).